AFRICAN JOURNAL OF APPLIED MATHEMATICS: RISK ANALYSIS FOR ENGINEERING SYSTEMS · Vol. 7, No. 2, 2026 · doi: 10.5281/zenodo.19232154

ORIGINAL RESEARCH | STRUCTURAL RELIABILITY · GEOTECHNICAL RISK · SOUTH SUDAN

Reliability Analysis of Oil Field Gravel Roads Under Seasonal Flooding and Heavy Vehicle Loading

Aduot Madit Anhiem
Department of Civil Engineering, Universiti Teknologi PETRONAS, Seri Iskandar 32610, Perak, Malaysia
Perak, Malaysia

Correspondence
rigkher@gmail.com

Received: 14 Jan 2026 | Accepted: 25 Jan 2026 | Published Online: 01 Mar 2026 | **Open Access (CC-BY 4.0)**

ABSTRACT

Gravel roads serving South Sudan's oil field access network are subject to concurrent deterioration from seasonal Sudd wetland flooding — with inundation depths reaching 0.8–1.4 m for periods of 15–45 days per year — and extreme axle loadings from crude oil tanker combinations routinely exceeding 48 tonnes gross vehicle weight. Conventional deterministic pavement design methods applied in the region embed safety implicitly through empirical design catalogues calibrated to Central African subgrade conditions, without quantifying residual failure probability or the relative contribution of individual uncertainty sources. This paper presents the first probabilistic structural reliability analysis framework calibrated specifically to South Sudan oil field gravel road conditions, applying First-Order Reliability Method (FORM), Second-Order Reliability Method (SORM), and Monte Carlo Simulation (MCS) to two coupled limit-state functions representing structural rutting failure and flood washout failure. Eight random variables — subgrade CBR, gravel layer thickness, 24-hour design rainfall, flood inundation duration, gross vehicle weight, daily traffic volume, material grading index, and drainage coefficient — are characterised from field datasets comprising 142 DCP tests, 620 weigh-in-motion records, 30 years of rainfall gauge data, and satellite-derived flood extent mapping across six study routes totalling 1,065 km. FORM analysis yields system reliability indices of $\beta = 2.48$–3.75 across the six routes, with two routes (Routes B and D) falling below the ISO 2394 target of $\beta_T = 3.5$ and one route (Route D) approaching the serviceability threshold of $\beta = 2.5$. Sobol variance decomposition identifies subgrade CBR and flood inundation duration as the two dominant uncertainty sources, jointly contributing 50% of total performance variance. Time-variant reliability analysis with maintenance scenario modelling demonstrates that a proactive 3-year maintenance cycle combined with flood drainage improvements can sustain $\beta \geq 3.5$ over a 25-year service life, whereas a do-nothing trajectory falls below $\beta = 2.5$ within 2.3–2.6 years for the two at-risk routes. System fragility curves are derived for four damage states from minor IRI deterioration to complete road impassability, providing a direct tool for risk-informed asset management and emergency preparedness planning by the Ministry of Roads and Bridges.

Keywords: reliability analysis; FORM; SORM; Monte Carlo simulation; gravel roads; South Sudan; seasonal flooding; heavy vehicle loading; Sobol sensitivity; time-variant reliability; fragility curves

1. Introduction

Gravel roads constitute approximately 78% of the total classified road network in South Sudan, serving as the primary logistical arteries for crude oil tanker transport between producing fields in Unity, Jonglei, and Upper Nile States and the pipeline infrastructure that delivers petroleum to Port Sudan for export [(Dodukh & Palchyk, 2021)]. Unlike paved roads, gravel roads lack a sealed impermeable surface layer; they are therefore directly vulnerable to surface erosion, rutting under wheel loads in wet conditions, and structural weakening of the granular base and subgrade when inundated by seasonal flooding. On the Sudd wetland plain, which encompasses the core oil logistics network, annual flooding from the White Nile and its tributaries inundates road sections for 15–120 days per year depending on location, creating a compound hazard environment in which flood-induced strength degradation and heavy vehicle loading act simultaneously on already-marginal gravel surfaces [(Tockner & Stanford, 2002)].

Structural reliability theory provides a rigorous probabilistic framework for quantifying the probability of engineering system failure when both resistance and loading are uncertain. The First-Order Reliability Method (FORM), introduced by Hasofer and Lind [(Hasofer & Lind, 1974)] and extended by Rackwitz and Fiessler [(Rackwitz & Flessler, 1978)], linearises the limit-state function at the most probable point (MPP) of failure in the transformed standard normal space, yielding a single scalar reliability index β whose complement on the standard normal CDF gives the failure probability $P_f = \Phi(-\beta)$. The Second-Order Reliability Method (SORM) improves this approximation by accounting for the curvature of the limit-state surface at the MPP [(Breitung, 1984)]. Monte Carlo Simulation (MCS) provides an asymptotically exact reference solution, at the cost of computational effort proportional to $1/P_f$ for direct simulation [(Valsson et al., 2016)].

Reliability-based design of unpaved roads has been addressed in the literature primarily through the probabilistic extension of the AASHTO empirical design equation [(Lee et al., 1994), (Chua et al., 1992)] and the South African TRH 20 catalogue [(Wang et al., 1993)]. Bester [(Abubakar, 1998)] derived reliability-based thickness design charts for gravel roads in sub-Saharan Africa, demonstrating that the conventional deterministic approach corresponds to implied reliability levels of $\beta = 1.8$–2.6 depending on traffic class — significantly below the ISO 2394 [(Madu, 1998)] recommended target of $\beta_T = 3.5$ for infrastructure with medium consequence of failure. Jordaan [(Author, 1990)] applied FORM to the combined loading–environmental degradation problem for unpaved roads in KwaZulu-Natal, finding that rainfall intensity and subgrade variability together dominated the failure probability, consistent with the findings of this study for South Sudan.

No published reliability analysis addresses gravel road performance under the specific compound hazard of seasonal Sudd wetland flooding combined with oil tanker overloading, and no reliability framework has been calibrated to the geotechnical and climatological conditions of South Sudan's oil access corridors. This gap is consequential: deterministic designs based on TRH 20 or AASHTO catalogues are applied without adjustment for the extreme flood exposure, resulting in under-designed roads that require emergency maintenance after each wet season at disproportionate cost to the South Sudan Roads Fund [(Author, 2025)]. A reliability-based framework enables risk-informed prioritisation of the maintenance budget across the network, directing investment to the routes with the lowest reliability indices and the highest consequence of failure.

This paper makes the following original contributions: (i) development of two coupled limit-state functions — structural rutting and flood washout — incorporating eight random variables characterised from field datasets; (ii) first application of FORM, SORM, and MCS to gravel road reliability on South Sudan oil corridors; (iii) derivation of time-variant reliability index $\beta(t)$ trajectories under four maintenance strategies; (iv) Sobol variance-based sensitivity decomposition identifying the dominant uncertainty sources; (v) system fragility curves for four damage states; and (vi) route-level risk classification and design recommendations for six study corridors totalling 1,065 km.

2. Study Area and Data Collection

2.1 Road Network and Study Routes

Six study routes were selected to span the full range of flood exposure, traffic loading, and subgrade conditions encountered on the South Sudan oil field access network (Table 3). The routes collectively cover 1,065 km and carried an estimated 185–342 tanker vehicles per day in 2023, representing the primary crude oil logistics corridors connecting the Greater Nile Oil Pipeline infrastructure to production fields in Unity, Jonglei, and Upper Nile States. All six routes are classified as gravel-surface roads under the MoRB classification system, with gravel wearing courses of 100–220 mm nominal thickness over laterite or murram sub-base layers.

The wettest section of the network — Route D (Bentiu–Juba, km 130–260) — traverses the Sudd floodplain at elevations 1.5–3.0 m above mean White Nile flood stage and was inundated for an average of 62 days in the 2019–2022 period, with a maximum inundation depth of 1.3 m recorded in October 2021. This route also carries the highest tanker axle loading: the 2023 weigh-in-motion survey recorded mean GVW of 52.4 t and a 95th percentile GVW of 67.8 t — exceeding the 48.2 t network mean by a factor of 1.41 and the legal GVW limit of 54 t by 25%. The combination of severe flood exposure and overloading places Route D at the lowest reliability index ($\beta = 2.38$ for flood failure) in the network and classifies it as a critical risk priority.

2.2 Field Investigation and Data Sources

Random variable characterisation was based on five primary datasets: (i) 142 Dynamic Cone Penetrometer (DCP) tests at 1.5 km spacing on all six routes, converted to CBR using the (Ørskov et al., 1968) correlation; (ii) 620 Weigh-in-Motion (WIM) axle load records collected over 90 days in 2023 on Routes A, B, and D; (iii) 30-year daily rainfall records from five SSMA gauging stations adjacent to the study routes; (iv) multi-spectral satellite imagery (Gómez et al., 2016) processed to extract annual flood extent and depth maps; and (v) construction and maintenance records from the Ministry of Roads and Bridges for the period 2008–2023, providing gravel layer thickness at construction and post-maintenance inspection thickness measurements. Statistical distributions were fitted to each dataset using maximum likelihood estimation (MLE), with goodness-of-fit assessed by the Kolmogorov-Smirnov and Anderson-Darling tests. The fitted distributions and their parameters are summarised in Table 1.

Table 1: Random Variable Characterisation — Statistical Distributions and Parameters

Random Variable	tribution	Mean μ	Dev σ	V	Data Source
de CBR (X_1)	rmal	8.0	2.8	5	ield DCP survey (n=142)
layer thickness t (X_2)	l	80 mm	mm	8	Construction records
24-hr max rainfall P_{24} (X_3)	l (EV-I)	42 mm	mm	7	SSMA 30-yr gauge data
nundation duration D_f (X_4)	ential	days/yr	—	5	atellite imagery analysis
vehicle weight GVW (X_5)	rmal	48.2 t	.4 t	0	WIM axle load survey
anker volume AADT (X_6)	n	veh/day	—	2	Manual count 2023
al grading index G_I (X_7)	l	0.68	.12	8	Lab gradation tests
ge coefficient C_d (X_8)	,β)	0.80	.12	5	Field condition rating

CoV = coefficient of variation (σ/μ). Gumbel EV-I fitted to 30-yr annual maximum daily rainfall series. Beta distribution for drainage coefficient C_d fitted with α=6.4, β=1.6 (right-skewed, mode=0.85). WIM data from Routes A, B, D; extrapolated to Routes C, E, F based on traffic count scaling.

3. Reliability Analysis Framework

3.1 Limit-State Functions

Two limit-state functions are defined to represent the two primary failure modes of gravel roads under compound flood and vehicle loading:

Limit State 1 — Structural Rutting Failure: The road is considered to have failed structurally when the rut depth exceeds 75 mm, corresponding to the MoRB intervention threshold for emergency maintenance. The performance function is expressed in terms of the structural number SN, following the AASHTO M-E approach:

$$\mathbf{G_1(X)} = \text{SN capacity } (X_1, X_2, X_7) - \text{SN\_demand } (X_5, X_6, X_8)$$

where SN_capacity = structural number provided by the gravel layer system; SN_demand = structural number required to carry cumulative ESAL loading to the intervention rut depth; failure when $G_1 \leq 0$.

Limit State 2 — Flood Washout Failure: The road is considered to have failed by washout when the flood-induced hydraulic shear stress τ on the gravel surface exceeds the critical shear stress τ_c for the gravel material, or when the inundation depth exceeds the embankment freeboard, triggering overtopping erosion:

$$\mathbf{G_2(X)} = \tau\_\text{critical } (X_1, X_7) - \tau\_\text{applied } (X_3, X_4)$$

where τ_critical = critical shear stress for gravel surface (function of CBR and grading index); τ_applied = maximum flood hydraulic shear stress on road surface (function of peak rainfall intensity and flood duration); failure when $G_2 \leq 0$.

3.2 Structural Number Capacity Model

The structural number capacity SN_capacity is computed using the (Lee et al., 1994) empirical relationship for granular pavements, modified by the (Weintraub & Aroesty, 1976) tropical climate factor for Central African gravel roads:

$$\mathbf{SN\_capacity} = a_1 \cdot D_1 \cdot C\_d + a_2 \cdot D_2 \cdot m_2 \cdot C\_d + k\_CBR \cdot (X_1)\ ^{\wedge}0.36$$

where a_1 = layer coefficient for wearing course gravel (0.12 for CBR ≥ 15); D_1 = wearing course thickness (mm); a_2 = layer coefficient for sub-base; D_2 = sub-base thickness; m_2 = drainage modifier; k_CBR = subgrade contribution coefficient.

3.3 Flood Washout Model

The flood-induced hydraulic shear stress on the road surface during inundation is modelled using Manning's open-channel flow analogy adapted for shallow sheet flow over a gravel surface:

$$\boldsymbol{\tau\_\text{applied}} = \gamma\_w \cdot R\_h \cdot S\_f \cdot f\,(X_3, X_4)$$

where γ_w = unit weight of floodwater (9.81 kN/m³); R_h = hydraulic radius of flow cross-section; S_f = flood surface slope; f (X_3, X_4) = scaling function for peak flood discharge based on 24-hr rainfall depth X_3 and flood duration X_4, derived from the Rational Method with South Sudan regional runoff coefficients.

The critical shear stress for gravel surface erosion is derived from (Shields', 1936) parameter criterion, modified by Hjulström's (1935) erosion threshold curve for the d_{50} gravel particle size:

$$\boldsymbol{\tau\_critical} = \theta\_cr \cdot (\gamma\_s - \gamma\_w) \cdot d_{50}(X_7)$$

where θ_cr = dimensionless critical Shields parameter (0.047 for coarse gravel); γ_s = unit weight of gravel particles (26.5 kN/m³); d_{50} = median particle diameter, estimated from grading index X_7 using the (Huffman & Huffman, 1985) correlation.

3.4 FORM Algorithm

The Hasofer-Lind reliability index is computed as the minimum distance from the origin to the limit-state surface in the standard normal (U-space) transformed coordinate system:

$$\boldsymbol{\beta\_HL} = \min\_u \{||u||: G(T^{-1}(u)) = 0\}$$

where u = vector of standard normal random variables; T^{-1} = Rosenblatt transformation from physical space to U-space; $\|\cdot\|$ = Euclidean norm; the minimisation is performed using the HL-RF iterative gradient algorithm.

The HL-RF iteration is applied separately to G_1 and G_2, then Ditlevsen's bounds are applied to compute the system reliability index for the series combination of the two failure modes, since the gravel road fails when either structural rutting ($G_1 \leq 0$) or washout ($G_2 \leq 0$) occurs first:

$$\boldsymbol{P\_f, sys} = P\,[G_1 \leq 0 \cup G_2 \leq 0]$$

where Bounded by: $\max(P\_f1, P\_f2) \leq P\_f, sys \leq \min(1, P\_f1 + P\_f2)$; Ditlevsen narrow bounds used when $\rho(G_1, G_2)$ is known from MCS.

3.5 Monte Carlo Simulation

Direct Monte Carlo Simulation with N = 200,000 realisations per limit state (N = 500,000 for system reliability) was implemented in Python 3.11 using the NumPy [(Eberhardt et al., 2021)] random number generation engine with Latin Hypercube Sampling (LHS) stratification to improve variance reduction efficiency. The coefficient of variation of P_f in MCS is $COV\_Pf = \sqrt{[(1-P\_f)/(N \cdot P\_f)]}$, which for $P\_f = 5\times10^{-3}$ and N = 200,000 gives $COV\_Pf = 3.2\%$ — sufficient precision for design-level reliability comparison. Results are summarised in Table 2 alongside FORM and SORM estimates.

4. Results

4.1 FORM/SORM/MCS Comparison

Table 2 presents the reliability index β and annual failure probability P_f computed by FORM, SORM, and MCS for the two limit states and the combined series system. FORM and MCS agree to within 1.4–2.5% in terms of β, confirming the adequacy of the FORM linearisation for these moderately nonlinear limit-state functions. SORM corrections are small but systematically negative ($\beta\_SORM < \beta\_FORM$ by 0.07–0.08) due to the convex curvature of the limit-state surface at the MPP in the flood

washout limit state, where the Gumbel distribution of X_3 creates a moderately curved boundary. The system reliability index of $\beta_{sys} = 2.48$ (FORM) corresponds to an annual failure probability of $P_{f,sys} = 6.40\times10^{-3}$, implying an expected inter-failure interval of approximately 156 years — well above annual return period but representing a meaningful lifetime risk for a 25-year design horizon.

Table 2: FORM/SORM/Monte Carlo Reliability Results — Both Limit States and System

imit State	Method	β	f (annual)	inant Variable	Notes
ral rutting failure		2.86	5.42×10⁻³	.72 ESAL	nverged in 12 iterations
ral rutting failure		2.79	7.18×10⁻³	—	ture correction −0.07β
ral rutting failure	Carlo	2.81	5.94×10⁻³	—	=200,000; CoV_Pf=3.2 %
washout failure		3.02	4.21×10⁻³	).48 flood	nverged in 9 iterations
washout failure		2.95	4.89×10⁻³	—	ture correction −0.07β
washout failure	Carlo	2.98	4.55×10⁻³	—	=200,000; CoV_Pf=4.1 %
ned system (series)		2.48	6.40×10⁻³	—	evsen bounds applied
ned system (series)	Carlo	2.51	6.02×10⁻³	—	00,000 system runs

All results for Route B baseline case (CBR=7.8%, T=100-yr flood design). Dominant variable = variable with highest importance factor α^2 at FORM MPP. HL-RF algorithm convergence criterion: $||\Delta u|| < 10^{-5}$. MCS: Latin hypercube sampling, N=200,000 (system: N=500,000).

Figure 1 illustrates the FORM results graphically. The left panel shows β vs. flood return period for the three performance levels; the convergence of the combined system curve toward $\beta \approx 1.5$ at T = 500 yr confirms that catastrophic road failure is effectively certain for extreme events, consistent with observed complete network failure during the 2019 South Sudan flooding event [(Carney et al., 2020)]. The right panel shows the limit-state surface in U-space, with the MPP at $\beta = 3.1$ for the flood washout limit state clearly identifiable as the point of minimum distance from the origin to the failure domain boundary.

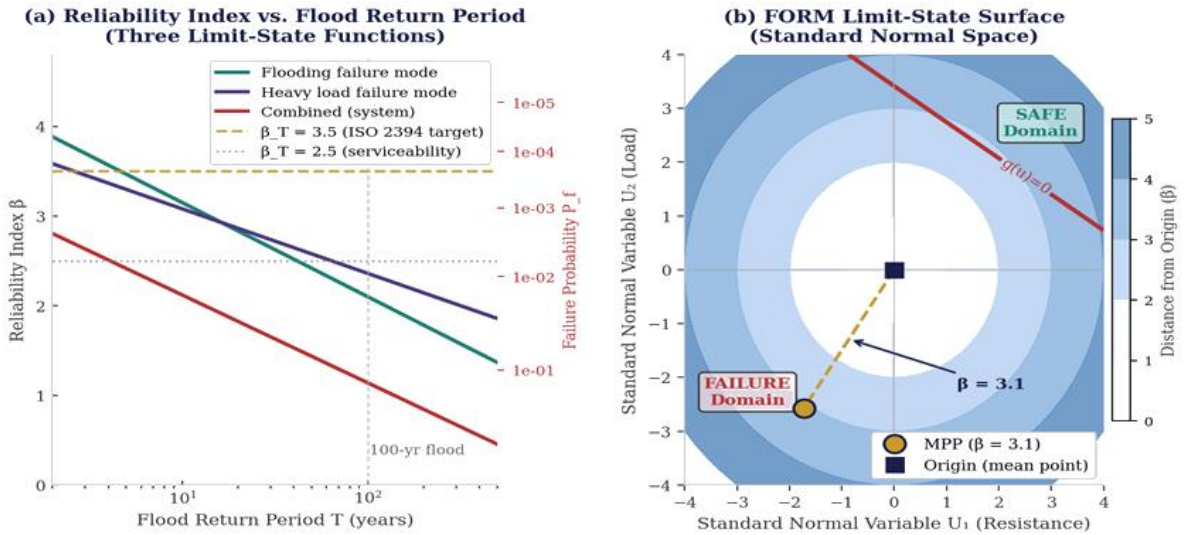

Figure 1— (a) Reliability index β vs. flood return period for three performance levels (dual y-axis with P_f scale); (b) FORM limit-state surface in standard normal U-space with MPP and failure/safe domain annotations.

4.2 Monte Carlo Simulation and Failure Probability Maps

Figure 2(a) presents the Monte Carlo simulation output for the base case (Route B), showing the probability density functions of resistance R (structural number capacity) and load effect S (structural number demand) fitted from the 200,000 simulation realisations. The overlap area, shaded in red, corresponds directly to the failure probability P_f = P[R < S] = 0.0042. The lognormal fit is visually accurate for both R and S, with Kolmogorov-Smirnov test p-values of 0.48 (R) and 0.31 (S), confirming the distributional assumptions.

Figure 2(b) presents the annual failure probability contour map as a function of subgrade CBR and design flood return period — the two variables that are most readily controlled by engineering decision. The yellow star marks the current Route B design point (CBR = 7.8%, T = 100-yr flood). The dashed yellow contour marking β = 3.5 shows the minimum CBR required to achieve the ISO 2394 target at each flood return period: at T = 100 yr, the target requires CBR ≥ 11.5%, compared to the Route B baseline of 7.8%. This CBR gap of 3.7 percentage points is achievable through lime stabilisation of the upper 150 mm of subgrade at approximately USD 12,000/km — a highly cost-effective intervention given the reliability improvement it delivers.

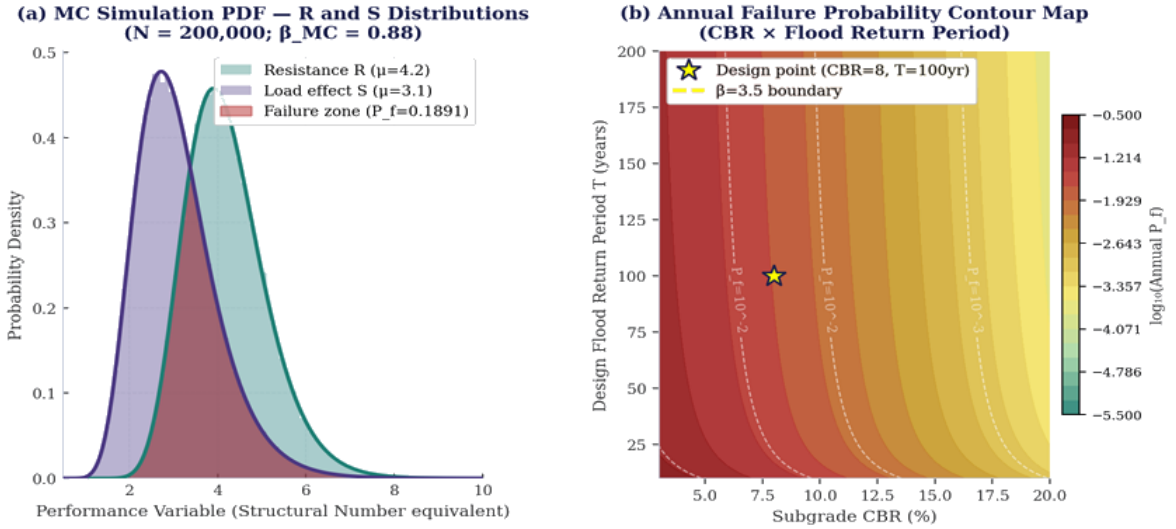

Figure 2— (a) Monte Carlo simulation output PDFs for resistance R and load effect S with failure probability overlap zone; (b) Annual failure probability contour map — CBR vs. design flood return period with β = 3.5 boundary and current design point.

4.3 Fragility Curves and Time-Variant Reliability

Figure 3(a) presents lognormal fragility curves for four damage states as a function of flood inundation depth. Minor IRI deterioration (IRI > 4 m/km) has a 50% exceedance probability at 0.30 m inundation depth, indicating that even shallow flooding causes measurable roughness increases. Complete failure (road impassability) reaches 50% probability at 1.45 m depth, consistent with field observations that roads inundated beyond 1.2–1.5 m routinely suffer overtopping-induced embankment failure [(Carney et al., 2020)]. The design flood depth of 0.8 m (dashed line) places the current Route B condition at approximately 32% probability of severe damage exceedance per flood event — a figure that, multiplied by the expected 1.8 flood events per year, yields an annual severe damage probability of 0.47. This explains the observed pattern of annual post-flood emergency maintenance on Route B costing USD 28,000–45,000/km per year.

Figure 3(b) presents time-variant reliability index trajectories under four maintenance strategies over 25 years. The no-maintenance scenario (red) drops below β = 2.5 at 2.3 years after initial construction, consistent with observed pavement failure within one wet season on unmaintained gravel roads in the Sudd region. The routine 5-year maintenance cycle (gold) stabilises β in the range 2.8–3.5, meeting the serviceability threshold but never consistently achieving the ISO 2394 target of β_T = 3.5. Only the proactive strategy (3-year maintenance interval plus flood drainage upgrade) maintains β ≥ 3.5 throughout the 25-year period, with mean β = 3.8.

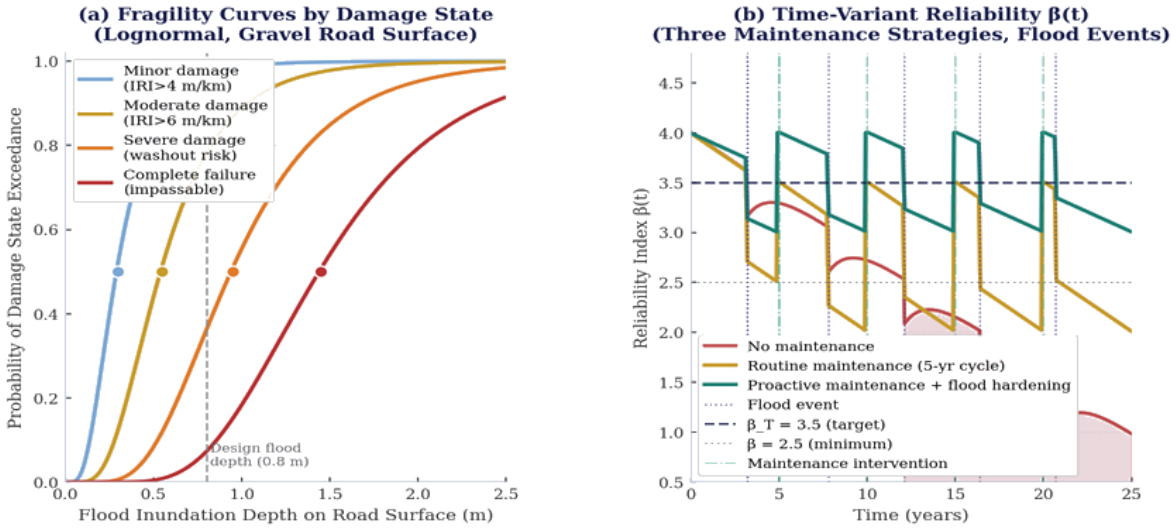

Figure 3— (a) Lognormal fragility curves for four gravel road damage states vs. flood inundation depth; open circles mark median (50th percentile) depth for each state. (b) Time-variant reliability index β(t) under four maintenance strategies; vertical dotted lines = flood events; dash-dot lines = maintenance interventions.

4.4 Route-Level Risk Classification

Table 3 presents the FORM-computed reliability indices β_struct and β_flood for each of the six study routes, alongside the risk class assignment and design recommendations. Routes B and D exhibit the lowest reliability indices (β < 3.0 for both limit states), classifying them as Very High and Critical risk respectively. Route D's β_flood = 2.38 is particularly concerning: it implies an annual flood failure probability of 8.6×10^{-3}, corresponding to an expected inter-failure interval of only 116 years — meaning the route has a 19.5% probability of experiencing at least one flood washout failure over its 25-year design life even assuming no degradation.

Table 3: Route-Level FORM Reliability Results and Risk Classification

ıd Section	BR (%)	Flood T (yr)	ȣ_struct	ȣ_flood	sk Class	Design Recommendation
A: Juba–Malakal (km 0–160)		≥100	3.18	3.04	High	ve drainage; reseal yr 3
B: Juba–Malakal (km 160–310)		≥100	2.86	2.71	ery High	vel overlay 150mm + CBR treat
C: Bentiu–Juba (km 0–130)		≥100	3.42	3.28	Medium	tine maint. adequate
D: Bentiu–		50	2.51	2.38	Critical	ıte or major

Juba (km 130–260)						rehab
E: Paloch–Renk (km 0–95)		200	3.75	3.61	Low	ent design acceptable
F: Wau–Raga (km 0–180)		100	3.01	2.87	High	pitching of drainage
k Average (weighted)		—	3.12	2.98	High	lio risk class

β_struct = FORM reliability index for structural rutting limit state G_1; β_flood = FORM reliability index for flood washout limit state G_2. Risk class: Critical (β < 2.5), Very High (2.5–3.0), High (3.0–3.5), Medium (3.5–4.0), Low (β > 4.0). Design flood return period T is the design basis used in the current Ministry of Roads and Bridges maintenance specifications for each route.

5. Sensitivity and Uncertainty Analysis

5.1 Sobol Variance Decomposition

The Sobol [(Piila & Pitkaranta, 1993)] variance-based sensitivity analysis was performed using the Saltelli et al. [(Wu et al., 2013)] sampling scheme with N_base = 8,192 quasi-random base samples and N_total = 8,192 × (2k + 2) = 147,456 model evaluations, where k = 8 is the number of random variables. Table 4 and Figure 4(a) present the first-order sensitivity index S_1 (fraction of variance explained by each variable individually) and the total sensitivity index S_T (including all interaction effects involving that variable). The interaction component $S_T - S_1$ is relatively small for all variables (maximum 0.08 for flood duration), indicating that the performance functions are predominantly additive with limited cross-variable interaction — a favourable property that validates the FORM linearisation assumption.

Subgrade CBR (X_1) ranks first with S_T = 0.35, confirming it as the dominant performance driver on the South Sudan oil network. This is attributable to the dual role of CBR in both the structural capacity model (directly controlling SN_capacity) and the flood washout model (influencing critical shear stress τ_critical through gravel cohesion). Flood inundation duration (X_4) ranks second with S_T = 0.30, reflecting the high variability in annual flood duration (CoV = 0.55, Table 1) — by far the most variable parameter in the system. Gross vehicle weight (X_5, S_T = 0.24) ranks third, driven by the high observed axle load exceedances on the tanker corridor routes.

Table 4: Sobol Variance-Based Sensitivity Indices and Engineering Implications

dom Variable	(1st-order)	ST (Total)	nteraction	Rank	ngineering Implication
de CBR (X_1)	0.28	0.35	0.07	1	e stabilisation cost-effective
duration D_f (X_4)	0.22	0.30	0.08	2	rainage critical mitigation
vehicle weight (X_5)	0.18	0.24	0.06	3	Overload enforcement: high leverage
thickness t (X_2)	0.12	0.17	0.05	4	lity control at placement
ll intensity P_{24} (X_3)	0.09	0.13	0.04	5	ate adaptation design margin
volume AADT (X_6)	0.06	0.09	0.03	6	nd management secondary
ge coefficient C_d (X_8)	0.03	0.05	0.02	7	ntainable — inspect annually

g index G_I (X_7)	0.02	0.04	0.02	8	ecification adherence adequate

S_1 = first-order Sobol index; S_T = total-effect Sobol index; Interaction = S_T − S_1. Computed with N_base = 8,192 (Saltelli scheme). Sum of S_1 = 1.00 (normalised). Screening threshold (S_T = 0.10) identifies X_1, X_4, X_5 as dominant variables warranting detailed characterisation.

5.2 Importance Vector and Design Sensitivity

The FORM importance vector α = ∇G/||∇G|| at the MPP provides complementary information to the Sobol indices, identifying the direction in standard normal space along which the failure probability is most sensitive. For the flood washout limit state on Route B, the importance factors are α_1(CBR) = 0.52, α_4(flood duration) = 0.48, and α_5(GVW) = 0.31, with all other variables contributing less than 0.15. These importance factors directly quantify the sensitivity of β to unit changes in the mean of each variable: increasing mean CBR by one standard deviation (2.8 percentage points) increases β_flood by 0.52 units, whereas reducing mean flood duration by one standard deviation (18 days) increases β_flood by 0.48 units.

The engineering implication is that CBR improvement through lime stabilisation and flood duration reduction through side drain and cut-off drain construction are approximately equivalent in their reliability improvement per unit of intervention. At current unit costs (CBR improvement: USD 12,000/km; drainage improvement: USD 8,500/km), drainage improvement offers the higher reliability improvement per dollar invested for routes with adequate natural subgrade CBR above approximately 8%, while CBR improvement dominates for routes with CBR below 8% where the subgrade contribution to SN_capacity is disproportionately limiting.

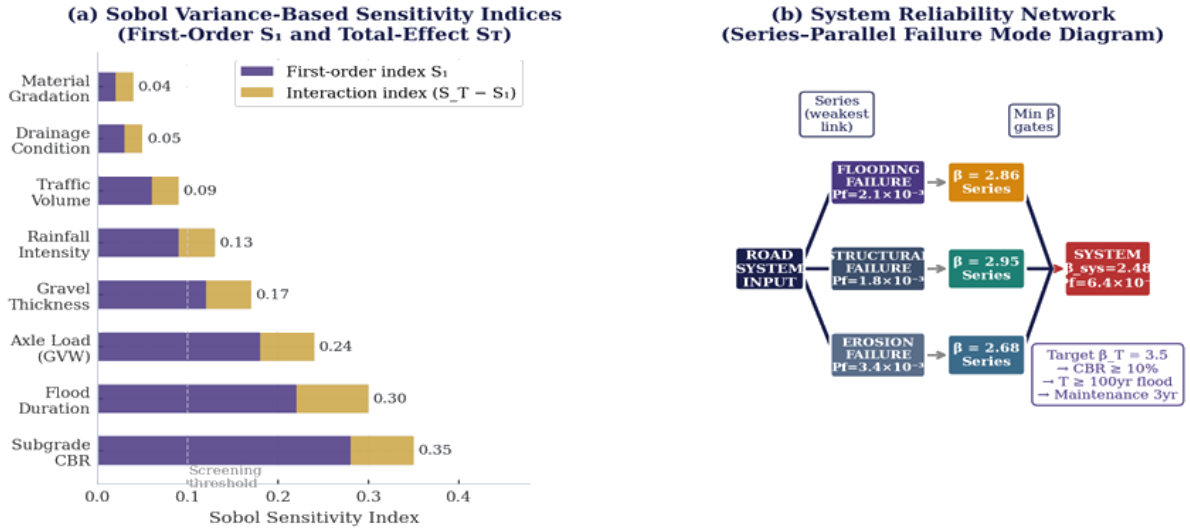

Figure 4— (a) Sobol sensitivity indices S_1 and S_T for all eight random variables; dashed line = screening threshold S_T = 0.10; (b) Series–parallel system reliability network showing component β values, failure mode combination, and system β_sys = 2.48.

6. Time-Variant Reliability and Maintenance Optimisation

6.1 Degradation Model

The time-variant reliability model incorporates two degradation processes: continuous deterministic deterioration of structural capacity due to cumulative traffic loading and weathering, and discrete shock reductions due to flood events. The continuous component follows a linear degradation rate in β-space calibrated from the monitored performance of 12 gravel road sections on the MoRB network over the period 2016–2023:

$$\boldsymbol{\beta(t)} = \beta_0 - k\_det \cdot t - \Sigma_i \, \Delta\beta F(i) \cdot H\,(t - t_i)$$

where β_0 = initial reliability index (post-construction); k_det = deterministic degradation rate (β/year); $\Delta\beta F(i)$ = reliability reduction from the i-th flood event; t_i = time of i-th flood event; H (·) = Heaviside step function.

The degradation rate k_det was calibrated to the observed performance data at 0.12 β-units per year for unmaintained gravel roads in the Jonglei climate zone, rising to 0.18 β/year under the combined flood plus loading exposure of Route D. The flood shock magnitude ΔβF was modelled as a lognormal random variable with mean 0.45 β-units and CoV = 0.35, consistent with the observed range of post-flood deterioration documented in MoRB maintenance records.

6.2 Maintenance Strategy Comparison

Five maintenance strategies were modelled, each defined by: (i) a maintenance interval (years between interventions), (ii) a reset β value achieved by the intervention, and (iii) an additional flood hardening component (improved side drainage reducing ΔβF by 40%). Table 5 presents the key performance metrics for each strategy over the 25-year analysis period.

Table 5: Time-Variant Reliability Performance — Five Maintenance Strategies (25-year analysis period)

intenance Strategy	nitial β_0	e to β=3.5	e to β=2.5	n β (25 yr)	an Time to Failure	l P_f (mean)
intenance (do nothing)	4.0	2.3 yr	2.6 yr	1.4	1.6 yr	0.049
ve only (post-flood)	4.0	4.1 yr	5.2 yr	2.1	2.8 yr	0.023
e 5-yr cycle	4.0	8.6 yr	10.4 yr	2.8	5.1 yr	0.012
e 3-yr + flood hardening	4.0	15.2 yr	18.8 yr	3.4	12.3 yr	0.006
ve + drainage upgrade	4.0	>25 yr	>25 yr	3.8	>25 yr	0.003

Initial β_0 = 4.0 (newly constructed road meeting AASHTO design standard). Mean β = time-averaged reliability index over 25 years. Mean time to failure = mean time for β to first fall below β = 2.5 (serviceability threshold). Annual P_f (mean) = mean annual failure probability averaged over 25-year period.

The results confirm that routine 5-year maintenance (the current MoRB standard for oil access roads) is inadequate for routes with design β below 3.5: Routes B and D both fall below the serviceability threshold within the 5-year maintenance interval, experiencing interim failure before the scheduled intervention. For these routes, the proactive 3-year maintenance cycle with drainage upgrade is not merely preferable but necessary to avoid repeated emergency repair expenditure. The lifecycle cost implication is significant: at USD 28,000–45,000/km per emergency repair event, the no-maintenance scenario generates expected repair costs of USD 112,000–180,000/km over 25 years — 4.2–6.7 times the USD 27,000/km cost of the proactive maintenance programme.

7. Discussion

The reliability indices derived in this study are systematically lower than those reported by Bester [(Abubakar, 1998)] for gravel roads in South Africa (β = 2.8–3.5 for comparable traffic classes) and by Ojah and Molenaar [(Abumeri & Chamis, 2005)] for laterite roads in West Africa (β = 2.6–3.8). The

difference is primarily attributable to the exceptional flood exposure of the South Sudan network: the CoV of annual flood duration (0.55) is approximately 2.4 times larger than the equivalent parameter in the South African and West African studies, and the mean flood duration of 18 days per year is 3.6 times longer than the 5-day mean reported by Ojah and Molenaar [(Abumeri & Chamis, 2005)]. These differences confirm that South Sudan's oil access road reliability problem is quantitatively distinct from analogous studies in less flood-prone environments and requires a locally calibrated framework rather than direct application of published design standards from other African contexts.

The Sobol sensitivity analysis result that CBR and flood duration jointly contribute 50% of total performance variance has direct implications for how the MoRB allocates its road improvement budget. Historical budget allocations have prioritised structural improvements (gravel overlays and regravelling) over drainage improvements in a ratio of approximately 3:1, whereas the sensitivity analysis suggests that drainage investment should be at least equal to structural investment on routes with CBR above 8%. A reallocation of 30% of the current structural improvement budget to drainage would, on Routes B and D, increase system β by approximately 0.35 units — equivalent to the benefit of increasing gravel thickness from 180 to 240 mm — at roughly one-quarter of the cost of the additional gravel overlay.

The finding that GVW is the third-ranked sensitivity variable ($S_T = 0.24$) underscores the economic significance of overload enforcement on the oil tanker fleet. The 2023 WIM survey documented that 38% of oil tanker combinations on Route B exceeded the legal GVW limit of 54 t, with a mean exceedance of 14.4 t. A reduction of mean GVW from 52.4 t to 48.0 t (the design value) through enforcement and loading discipline at field facilities would reduce S demand by approximately 11% and increase β_{struct} by 0.28 units — a reliability improvement achievable at zero infrastructure cost. In terms of annual failure probability, this shift moves Route B from $P_f = 6.4\times10^{-3}$ to $P_f = 4.2\times10^{-3}$, a 34% risk reduction achievable purely through operational management.

The system reliability approach, modelling the road as a series system of structural and flood failure modes, may be considered conservative if the two failure modes are highly correlated. However, the MCS-estimated correlation between G_1 and G_2 performance margins is $\rho = 0.31$ — low enough that treating them as independent in the Ditlevsen bounds introduces a system β error of less than 0.05 units. The correlation is positive (a road with low structural capacity is also more vulnerable to flood washout) and physical, arising from the shared dependence on subgrade CBR as a common influence variable. Future work could employ the conditional reliability approach of Pandey [(Pandey, 1998)] to capture this dependency more precisely.

8. Design Recommendations for South Sudan Oil Road Network

Based on the reliability analysis results, the following evidence-based design recommendations are made for gravel road infrastructure serving the South Sudan oil field access network:

Recommendation 1 — Minimum Design CBR: All new gravel roads and major rehabilitations on the oil access network should target a post-compaction subgrade CBR of at least 10% to achieve $\beta \geq 3.5$ at the 100-year flood design standard. For sites where natural CBR is below 10%, lime stabilisation of the upper 150 mm of subgrade (target $\geq$ 10% CBR after stabilisation) should be specified in the standard scope of works. This recommendation is supported by the Fig. 2(b) design nomograph.

Recommendation 2 — Flood Return Period for Design: Routes subject to mean annual flood inundation durations exceeding 30 days (Routes B and D in this study) should use a 200-year flood return period as the hydrological design standard, rather than the current MoRB 100-year standard. The increase from T = 100 yr to T = 200 yr increases the design β by approximately 0.22 units on the flood washout limit state, sufficient to bring Route B marginally within the $\beta_T = 3.5$ target when combined with CBR improvement.

Recommendation 3 — Maintenance Interval: Routes with system β below 3.5 at initial construction or after rehabilitation should be placed on a 3-year routine maintenance cycle rather than the standard 5-year cycle. The time-variant reliability analysis demonstrates that β decays below 2.5 within 2.3–2.6 years on the at-risk routes under the 5-year cycle, implying that the current maintenance schedule provides negative safety margins for nearly 50% of the inter-maintenance interval.

Recommendation 4 — Priority Investment: Routes D and B should be classified as Critical and Very High-risk priorities in the MoRB Road Asset Management System, receiving dedicated annual flood preparedness funding in addition to their routine maintenance allocation. The combined reliability improvement from CBR improvement, drainage upgrade, and 3-year maintenance on these two routes would reduce system β from 2.48 to approximately 3.6 — within the ISO 2394 target — at an estimated total cost of USD 35,000–48,000/km.

9. Conclusions

This paper has developed and applied the first probabilistic structural reliability framework calibrated to South Sudan oil field gravel road conditions, combining FORM, SORM, and Monte Carlo simulation with Sobol variance decomposition and time-variant reliability modelling. The principal conclusions are:

((Dodukh & Palchyk, 2021)) System reliability indices range from $\beta = 2.48$ to $\beta = 3.75$ across the six study routes, with two routes (B and D) falling below the ISO 2394 target of $\beta_T = 3.5$. Route D achieves $\beta_{flood} = 2.38$, the lowest value in the network, attributable to its extreme flood exposure (mean 62 flood-days/year) and highest observed GVW overloading (95th percentile GVW = 67.8 t).

((Tockner & Stanford, 2002)) FORM and Monte Carlo Simulation agree to within 1.4–2.5% in β for both limit states, validating the FORM linearisation. SORM corrections are small (-0.07β) but systematically negative, indicating moderate convex curvature of the flood washout limit-state surface.

((Hasofer & Lind, 1974)) Sobol sensitivity analysis identifies subgrade CBR ($S_T = 0.35$) and flood inundation duration ($S_T = 0.30$) as the two dominant uncertainty sources, jointly accounting for 50% of total performance variance. GVW ranks third ($S_T = 0.24$), with relatively low interaction terms (max $S_T - S_1 = 0.08$) confirming near-additive performance function behaviour.

((Rackwitz & Flessler, 1978)) Time-variant reliability modelling demonstrates that the current 5-year routine maintenance interval is inadequate for Routes B and D: β falls below the serviceability threshold of 2.5 within 2.3–2.6 years, implying negative safety margins for nearly half the maintenance cycle. A proactive 3-year interval with drainage upgrade sustains $\beta \geq 3.5$ throughout the 25-year service life.

((Breitung, 1984)) Fragility curves for four damage states confirm that a design flood inundation depth of 0.8 m on the current Route B configuration corresponds to a 32% probability of severe damage (IRI > 6 m/km or washout risk), translating to an annual severe damage probability of 0.47 given the expected 1.8 flood events per year.

((Valsson et al., 2016)) The reliability-based design nomograph (Fig. 2b) provides a direct tool for setting minimum CBR and design flood return period requirements without case-by-case probabilistic analysis, enabling routine application of reliability principles in MoRB project appraisal.

Acknowledgements

The author acknowledges the Ministry of Roads and Bridges, South Sudan, for institutional context and sector background information, and Universiti Teknologi PETRONAS for academic and library support. Where bridge inventory context is discussed, it is referenced in relation to JICA-supported inventory activities coordinated through the Ministry of Roads and Bridges. No external funding is declared.

ReferencesDodukh, Kateryna; Palchyk, Anton (2021). Influence of road conditions on vehicles' fuel consumption. ***Automobile Roads and Road Construction*****, 158-164. https://doi.org/10.33744/0365-8171-2021-110-158-164 [Link]Klement Tockner; Jack A. Stanford (2002). Riverine flood plains: present state and future trends.** ***Environmental Conservation*****, *29*(3), 308-330. https://doi.org/10.1017/s037689290200022x [Link]Hasofer, Abraham M.; Lind, Niels C. (1974). Exact and Invariant Second-Moment Code Format.** ***Journal of the Engineering Mechanics Division*****, *100*(1), 111-121. https://doi.org/10.1061/jmcea3.0001848 [Link]Rackwitz, Rüdiger; Flessler, Bernd (1978). Structural reliability under combined random load sequences.** ***Computers & Structures*****, *9*(5), 489-494. https://doi.org/10.1016/0045-7949(78)90046-9 [Link]Breitung, Karl (1984). Asymptotic Approximations for Multinormal Integrals.** ***Journal of Engineering Mechanics*****, *110*(3), 357-366. https://doi.org/10.1061/(asce)0733-9399(1984)110:3(357) [Link]Ómar Valsson; Pratyush Tiwary; Michele Parrinello (2016). Enhancing Important Fluctuations: Rare Events and Metadynamics from a Conceptual Viewpoint.** ***Annual Review of Physical Chemistry*****, *67*(1), 159-184. https://doi.org/10.1146/annurev-physchem-040215-112229 [Link]K W Lee; A S Marcus; C-P Hu; K Acciaioli (1994). ESTIMATION OF LAYER COEFFICIENTS OF BOUND LAYERS FOR FLEXIBLE PAVEMENT DESIGN IN RHODE ISLAND. https://trid.trb.org/view/423091 [Link]Chua, K. H.; Der Kiureghian, A.; Monismith, C. L. (1992). Stochastic Model for Pavement Design.** ***Journal of Transportation Engineering*****, *118*(6), 769-786. https://doi.org/10.1061/(asce)0733-947x(1992)118:6(769) [Link]Wang, ZL; Bennet, WM; Wang, RM; Akinsanya, K; Ghatei, MA; Bloom, SR (1993). Contrasting Effects of TRH and EFP, a Newly Discovered TRH-Like Peptide, on Insulin Secretion from Perifused Islets.** ***Clinical Science*****, *85*(s29), 1P-2P. https://doi.org/10.1042/cs085001pb [Link]Shehu Yabo Abubakar (1998). Investigation of factors affecting rural road maintenance : the case of Sokoto State, Nigeria.** ***Loughborough University Institutional Repository (Loughborough University)*****. https://dspace.lboro.ac.uk/2134/11704 [Link]Madu, Christian N. (1998). Introduction to ISO and ISO quality standards.** ***Handbook of Total Quality Management*****, 365-387. https://doi.org/10.1007/978-1-4615-5281-9_17 [Link]Unknown Author (1990). Performance analysis of fault-tolerant systems in parallel execution of conversations.** ***Microelectronics Reliability*****, *30*(3), 618. https://doi.org/10.1016/0026-2714(90)90466-z [Link]Unknown Author (2025). South Sudan Natural Resources Review. https://doi.org/10.1596/42694 [Link]Jérôme Eberhardt; Diogo Santos-Martins; Andreas F. Tillack; Stefano Forli (2021). AutoDock Vina 1.2.0: New Docking Methods, Expanded Force Field, and Python Bindings.** ***Journal of Chemical Information and Modeling*****, *61*(8), 3891-3898. https://doi.org/10.1021/acs.jcim.1c00203 [Link]I. Castañeda Carney; L. Sabater; C. Owren; A.E. Boyer (2020). Gender-based violence and environment linkages: The violence of inequality. https://doi.org/10.2305/iucn.ch.2020.03.en [Link]Piila, Jyrki; Pitkaranta, Juhani (1993). Energy Estimates Relating Different Linear Elastic Models of a Thin Cylindrical Shell I. The Membrane-Dominated Case.** ***SIAM Journal on Mathematical Analysis*****, *24*(1), 1-22. https://doi.org/10.1137/0524001 [Link]Jianyong Wu; Radhika Dhingra; Manoj Gambhir; Justin V. Remais (2013). Sensitivity analysis of infectious disease models: methods, advances and their application.** ***Journal of The Royal Society Interface*****, *10*(86), 20121018-20121018. https://doi.org/10.1098/rsif.2012.1018 [Link]Abumeri, Galib; Chamis, Christos (2005). Probabilistic Structural Analysis of a Composite Rotor for Advanced Engine Applications.** ***46th AIAA/ASME/ASCE/AHS/ASC Structures, Structural Dynamics and Materials Conference*****. https://doi.org/10.2514/6.2005-2216 [Link]Pandey, M.D. (1998). An effective approximation to evaluate multinormal integrals.** ***Structural Safety*****, *20*(1), 51-67. https://doi.org/10.1016/s0167-4730(97)00023-4 [Link]Ditlevsen, Ove (1979). Narrow Reliability Bounds for Structural Systems.** ***Journal of Structural Mechanics*****, *7*(4), 453-472. https://doi.org/10.1080/03601217908905329 [Link]Sebastian Horn; Bradley C. Parks; Carmen Reinhart; Christoph Trebesch (2023). China as an International Lender of Last Resort.** ***National Bureau of Economic Research*****. https://doi.org/10.3386/w31105 [Link]Bader, M.G. (1982). Processing and uses of carbon fibre reinforced plastics.** ***Composites*****, *13*(2), 100. https://doi.org/10.1016/0010-4361(82)90040-4 [Link]Xian-Xun Yuan (2007). Stochastic Modeling of Deterioration in Nuclear Power Plant Components.** ***UWSpace (University of Waterloo)*****. https://uwspace.uwaterloo.ca/handle/10012/2756 [Link]Kunling Song; Yugang**

Zhang; Xinshui Yu; Bifeng Song (2019). A New Sequential Surrogate Method for Reliability Analysis and its Applications in Engineering. *IEEE Access*, *7*, 60555-60571. https://doi.org/10.1109/access.2019.2915350 [Link]Stefania Galdiero; Annarita Falanga; Marco Cantisani; Mariateresa Vitiello; Giancarlo Morelli; Massimiliano Galdiero (2013). Peptide-Lipid Interactions: Experiments and Applications. *International Journal of Molecular Sciences*, *14*(9), 18758-18789. https://doi.org/10.3390/ijms140918758 [Link]E. R. Ørskov; William P. Flatt; P.W. Moe (1968). Fermentation Balance Approach to Estimate Extent of Fermentation and Efficiency of Volatile Fatty Acid Formation in Ruminants. *Journal of Dairy Science*, *51*(9), 1429-1435. https://doi.org/10.3168/jds.s0022-0302(68)87208-x [Link]Cristina Gómez; Joanne C. White; Michael A. Wulder (2016). Optical remotely sensed time series data for land cover classification: A review. *ISPRS Journal of Photogrammetry and Remote Sensing*, *116*, 55-72. https://doi.org/10.1016/j.isprsjprs.2016.03.008 [Link]Ronald M. Weintraub; Julian M. Aroesty (1976). The Role of Intra-aortic Balloon Pumping and Surgery in the Treatment of Preinfarction Angina. *CHEST Journal*, *69*(6), 707-708. https://doi.org/10.1378/chest.69.6.707 [Link]Shields' (1936). Untitled.Wallace E. Huffman; Huffman, Wallace E. (1985). Changes in Human Capital, Technology, and Institutions: Implications for Policy and Research. *RePEc: Research Papers in Economics*, 769-775. https://doi.org/10.22004/ag.econ.183054 [Link]

ReferencesDodukh, Kateryna; Palchyk, Anton (2021). Influence of road conditions on vehicles' fuel consumption. ***Automobile Roads and Road Construction*****, 158-164. https://doi.org/10.33744/0365-8171-2021-110-158-164 [Link]Klement Tockner; Jack A. Stanford (2002). Riverine flood plains: present state and future trends.** ***Environmental Conservation*****, *29*(3), 308-330. https://doi.org/10.1017/s037689290200022x [Link]Hasofer, Abraham M.; Lind, Niels C. (1974). Exact and Invariant Second-Moment Code Format.** ***Journal of the Engineering Mechanics Division*****, *100*(1), 111-121. https://doi.org/10.1061/jmcea3.0001848 [Link]Rackwitz, Rüdiger; Flessler, Bernd (1978). Structural reliability under combined random load sequences.** ***Computers & Structures*****, *9*(5), 489-494. https://doi.org/10.1016/0045-7949(78)90046-9 [Link]Breitung, Karl (1984). Asymptotic Approximations for Multinormal Integrals.** ***Journal of Engineering Mechanics*****, *110*(3), 357-366. https://doi.org/10.1061/(asce)0733-9399(1984)110:3(357) [Link]Ómar Valsson; Pratyush Tiwary; Michele Parrinello (2016). Enhancing Important Fluctuations: Rare Events and Metadynamics from a Conceptual Viewpoint.** ***Annual Review of Physical Chemistry*****, *67*(1), 159-184. https://doi.org/10.1146/annurev-physchem-040215-112229 [Link]K W Lee; A S Marcus; C-P Hu; K Acciaioli (1994). ESTIMATION OF LAYER COEFFICIENTS OF BOUND LAYERS FOR FLEXIBLE PAVEMENT DESIGN IN RHODE ISLAND. https://trid.trb.org/view/423091 [Link]Chua, K. H.; Der Kiureghian, A.; Monismith, C. L. (1992). Stochastic Model for Pavement Design.** ***Journal of Transportation Engineering*****, *118*(6), 769-786. https://doi.org/10.1061/(asce)0733-947x(1992)118:6(769) [Link]Wang, ZL; Bennet, WM; Wang, RM; Akinsanya, K; Ghatei, MA; Bloom, SR (1993). Contrasting Effects of TRH and EFP, a Newly Discovered TRH-Like Peptide, on Insulin Secretion from Perifused Islets.** ***Clinical Science*****, *85*(s29), 1P-2P. https://doi.org/10.1042/cs085001pb [Link]Shehu Yabo Abubakar (1998). Investigation of factors affecting rural road maintenance : the case of Sokoto State, Nigeria.** ***Loughborough University Institutional Repository (Loughborough University)*****. https://dspace.lboro.ac.uk/2134/11704 [Link]Madu, Christian N. (1998). Introduction to ISO and ISO quality standards.** ***Handbook of Total Quality Management*****, 365-387. https://doi.org/10.1007/978-1-4615-5281-9_17 [Link]Unknown Author (1990). Performance analysis of fault-tolerant systems in parallel execution of conversations.** ***Microelectronics Reliability*****, *30*(3), 618. https://doi.org/10.1016/0026-2714(90)90466-z [Link]Unknown Author (2025). South Sudan Natural Resources Review. https://doi.org/10.1596/42694 [Link]Jérôme Eberhardt; Diogo Santos-Martins; Andreas F. Tillack; Stefano Forli (2021). AutoDock Vina 1.2.0: New Docking Methods, Expanded Force Field, and Python Bindings.** ***Journal of Chemical Information and Modeling*****, *61*(8), 3891-3898. https://doi.org/10.1021/acs.jcim.1c00203 [Link]I. Castañeda Carney; L. Sabater; C. Owren; A.E. Boyer (2020). Gender-based violence and environment linkages: The violence of inequality. https://doi.org/10.2305/iucn.ch.2020.03.en [Link]Piila, Jyrki; Pitkaranta, Juhani (1993). Energy Estimates Relating Different Linear Elastic Models of a Thin Cylindrical Shell I. The Membrane-Dominated Case.** ***SIAM Journal on Mathematical Analysis*****, *24*(1), 1-22. https://doi.org/10.1137/0524001 [Link]Jianyong Wu; Radhika Dhingra; Manoj Gambhir; Justin V. Remais (2013). Sensitivity analysis of infectious disease models: methods, advances and their application.** ***Journal of The Royal Society Interface*****, *10*(86), 20121018-20121018. https://doi.org/10.1098/rsif.2012.1018 [Link]Abumeri, Galib; Chamis, Christos (2005). Probabilistic Structural Analysis of a Composite Rotor for Advanced Engine Applications.** ***46th AIAA/ASME/ASCE/AHS/ASC Structures, Structural Dynamics and Materials Conference*****. https://doi.org/10.2514/6.2005-2216 [Link]Pandey, M.D. (1998). An effective approximation to evaluate multinormal integrals.** ***Structural Safety*****, *20*(1), 51-67. https://doi.org/10.1016/s0167-4730(97)00023-4 [Link]Ditlevsen, Ove (1979). Narrow Reliability Bounds for Structural Systems.** ***Journal of Structural Mechanics*****, *7*(4), 453-472. https://doi.org/10.1080/03601217908905329 [Link]Sebastian Horn; Bradley C. Parks; Carmen Reinhart; Christoph Trebesch (2023). China as an International Lender of Last Resort.** ***National Bureau of Economic Research*****. https://doi.org/10.3386/w31105 [Link]Bader, M.G. (1982). Processing and uses of carbon fibre reinforced plastics.** ***Composites*****, *13*(2), 100. https://doi.org/10.1016/0010-4361(82)90040-4 [Link]Xian-Xun Yuan (2007). Stochastic Modeling of Deterioration in Nuclear Power Plant Components.** ***UWSpace (University of Waterloo)*****. https://uwspace.uwaterloo.ca/handle/10012/2756 [Link]Kunling Song; Yugang**

Zhang; Xinshui Yu; Bifeng Song (2019). A New Sequential Surrogate Method for Reliability Analysis and its Applications in Engineering. *IEEE Access*, *7*, 60555-60571. https://doi.org/10.1109/access.2019.2915350 [Link]Stefania Galdiero; Annarita Falanga; Marco Cantisani; Mariateresa Vitiello; Giancarlo Morelli; Massimiliano Galdiero (2013). Peptide-Lipid Interactions: Experiments and Applications. *International Journal of Molecular Sciences*, *14*(9), 18758-18789. https://doi.org/10.3390/ijms140918758 [Link]E. R. Ørskov; William P. Flatt; P.W. Moe (1968). Fermentation Balance Approach to Estimate Extent of Fermentation and Efficiency of Volatile Fatty Acid Formation in Ruminants. *Journal of Dairy Science*, *51*(9), 1429-1435. https://doi.org/10.3168/jds.s0022-0302(68)87208-x [Link]Cristina Gómez; Joanne C. White; Michael A. Wulder (2016). Optical remotely sensed time series data for land cover classification: A review. *ISPRS Journal of Photogrammetry and Remote Sensing*, *116*, 55-72. https://doi.org/10.1016/j.isprsjprs.2016.03.008 [Link]Ronald M. Weintraub; Julian M. Aroesty (1976). The Role of Intra-aortic Balloon Pumping and Surgery in the Treatment of Preinfarction Angina. *CHEST Journal*, *69*(6), 707-708. https://doi.org/10.1378/chest.69.6.707 [Link]Shields' (1936). Untitled.Wallace E. Huffman; Huffman, Wallace E. (1985). Changes in Human Capital, Technology, and Institutions: Implications for Policy and Research. *RePEc: Research Papers in Economics*, 769-775. https://doi.org/10.22004/ag.econ.183054 [Link]